X-621-72-185
PREPRINT

NASA TM X- 65928

# THE DIURNAL HEAT BUDGET OF THE THERMOSPHERE

**S. CHANDRA**
**A. K. SINHA**

(NASA-TM-X-65928) THE DIURNAL HEAT BUDGET OF THE THERMOSPHERE S. Chandra, et al (NASA) May 1972 29 p CSCL 04A

N72-27364

Unclas
G3/13 34242

MAY 1972

GSFC — GODDARD SPACE FLIGHT CENTER
GREENBELT, MARYLAND

Reproduced by
NATIONAL TECHNICAL
INFORMATION SERVICE
U S Department of Commerce
Springfield VA 22151

X-621-72-185
Preprint

# THE DIURNAL HEAT BUDGET OF THE THERMOSPHERE

S. Chandra
Laboratory for Planetary Atmospheres
Goddard Space Flight Center
Greenbelt, Maryland 20771

A. K. Sinha
Institute for Fluid Dynamics and Applied Mathematics
University of Maryland
College Park, Maryland

May 1972

GODDARD SPACE FLIGHT CENTER
Greenbelt, Maryland

# THE DIURNAL HEAT BUDGET OF THE THERMOSPHERE

S. Chandra
Laboratory for Planetary Atmospheres
Goddard Space Flight Center
Greenbelt, Maryland 20771

A. K. Sinha
Institute for Fluid Dynamics and Applied Mathematics
University of Maryland
College Park, Maryland

## ABSTRACT

Detailed numerical calculations of thermospheric heat sources and sinks are presented and their relative importance is discussed in reference to the energy balance phenomena of the neutral atmosphere. It is shown that the thermal energy available from the absorption in the Schumann-Runge continuum leading to photo-dissociation of $O_2$ is by far the largest energy source in the lower thermosphere. Other sources of varying importance in different altitude ranges are: (1) energy from photoelectrons; (2) energy exchange from thermal plasma; (3) chemical reactions (ion-electron dissociative recombination) energy gain; (4) kinetic and dissipative energy associated with the neutral wind. The energy sinks of importance are (1) thermal conduction at the lower boundary (120 km); and (2) radiative cooling of atomic oxygen.

It is shown that the combined energy from processes 2-4 constitute only a small fraction of the total energy available from photoelectrons and are in phase with the latter. These secondary sources (processes 2-4), therefore, do not

constitute a significant energy source and their contribution can be simply incorporated into photoelectron energy (process 1) by defining an effective photoionization heating efficiency. The heating efficiencies for photoionization (including processes 2-4) and photo-dissociation are estimated to be 0.5 and 0.3, respectively.

As the important heat input (photo-dissociation) and loss (conduction and radiation) rates are basically governed by the $O_2$ and O densities, any diurnal or seasonal variation in these constituents at the lower boundary would have profound effects on the thermal structure of the overlying atmosphere. For this and other reasons, it is suggested that a choice of lower boundary much below 120 km, e.g. near the mesopause level (90 km), should be more appropriate for general thermospheric studies.

# THE DIURNAL HEAT BUDGET OF THE THERMOSPHERE

## INTRODUCTION

The purpose of this paper is to study the diurnal heat budget problem of the thermosphere and discuss the relative importance of the various heat sources which influence the thermal structure of the upper atmosphere. These heat sources, which are the result of the photochemical and dynamical processes, derive their energy from the sun, primarily from the ultraviolet and far ultraviolet region of the solar spectrum.

In solving the energy balance equation for the thermospheric region, it has been customary to represent the heat input term by multiplying the absorbed solar ultraviolet energy with a constant factor, often referred to as a heating efficiency [Harris and Priester, 1962; Lagos and Mahoney, 1967; Chandra and Stubbe, 1970; Izakov, 1971]. Though the estimate of the heating efficiency varied over a wide range, from 0.1-0.6 [Nicolet (1961), Hanson and Johnson (1961), Hunt and Van Zandt (1961), Lazarev (1963)] and the various authors used values most suited to them, the concept of heating efficiency was useful in providing a short-cut alternative to a laborious calculation of multiple-channel energy and radiative transfer problem. On the other hand, the heating efficiency became a convenient scapegoat for our lack of understanding of many of the problems which arose as a result of our increasing knowledge of the thermospheric structure.

The difficulty in defining an effective heating efficiency is compounded by the fact that the various aeronomic processes which contribute to the heating of the thermosphere have different time constants. For example, the various ions which are produced as a result of photo-ionization are transported to different regions (as a result of dynamical and diffusion processes) before recombining. These recombination processes are exothermic and therefore they constitute a chemical heat source. Similarly the thermal plasma, which is usually at a higher temperature than the neutral gas, imparts some of its energy to the latter as a result of elastic and inelastic collisions. Likewise both the thermal plasma and the neutral gas, as a result of their mutual interaction, share some of the kinetic energy associated with the neutral wind (generated as a result of the global pressure gradients). Because of the complex coupling of the various processes, a realistic assessment of their relative importance can only be made by solving the system of basic ionospheric and atmospheric equations simultaneously in a self-consistent manner. This paper is an approach in that direction.

## HEAT INPUT RATES

Basic physical processes considered here are as follows:

(i) photo-ionization of neutral constituents ($O$, $O_2$, $N_2$).

(ii) photo-dissociation of $O_2$ in the Schumann-Runge continuum.

(iii) electron-ion recombination (chemical heating).

(iv) thermal energy transfer from electrons and ions to the neutrals.

(v) neutral wind (ion-drag).

(vi) infrared radiation loss.

A brief discussion of these processes in the context of neutral heating and the method of their calculation are given below. The results of calculation are presented in the next section.

## PHOTOIONIZATION

Solar radiation in EUV and x-ray ranges ionizes the major neutral constituents ($N_2$, $O_2$, O) and photon energy in excess of the respective ionization threshold is transferred to electron-ion pair created. Kinetic energy is mostly carried by light photoelectrons (against massive ions), which subsequently lose their energy to the thermal electrons through Coulomb collisions and to the neutral gas through elastic, superelastic and inelastic collisions. In general, however, the ions are created in different excited states and the actual energy available to the photoelectrons is less than the excess photon energy over the ionization threshold. Some loss or gain of photoelectron energy may also occur due to their transport to or from the conjugate hemisphere — an effect especially important during pre-dawn and post-sunset conditions. The total thermal energy available to the neutral gas after photoionization may, therefore, be calculated from the following expression

$$Q_i = \sum_{k,j} \int_{\lambda < 1250\,\mathrm{\mathring{A}}} \sigma_{j\lambda}^{i}\, n_j(z)\, (\epsilon_\lambda - \epsilon_j^{i} - \epsilon_{kj} P_{kj\lambda}) \{1 - f_\lambda^{e}(z) - f_\lambda^{O(^1D)}(z)\} \frac{F_{\lambda\infty}}{\epsilon_\lambda} e^{-\tau_\lambda(z)}\, d\lambda \tag{1.a}$$

where

$$\tau_\lambda(z) = \text{Optical depth} = \sum_j \sigma_{j\lambda}^{a} \cdot \int_{z_\infty}^{z} Ch(\chi)\, n_j(z)\, dz \tag{1.b}$$

$n_j(z)$ = Number density of the neutral species j at altitude z.

$\sigma_{j\lambda}^{i}$ = photo-ionization cross section of species j in the wavelength range $\lambda$ to $\lambda + d\lambda$.

$\sigma_{j\lambda}^{a}$ = absorption cross section of species j in the wavelength range $\lambda$ to $\lambda + d\lambda$.

$\epsilon_\lambda$ = energy of a photon with wavelength $\lambda$ ($\epsilon_\lambda = \frac{hc}{\lambda}$, where h = Planck's constant and c = velocity of light)

$\epsilon_j^i$ = ionization threshold of the species j.

$\epsilon_{kj}$ = internal energy of the kth excited level of an ion from species j.

$P_{kj\lambda}$ = probability of production of kth excited ionic state during photo-ionization of the species j by a photon of wavelength $\lambda$.

$Ch(\chi)$ = Chapman function ($\chi$ = solar zenith angle).

$F_{\lambda\infty}$ = exospheric photon energy flux in the wavelength range $\lambda$ and $\lambda + d\lambda$.

$f_\lambda^e$ = fraction of photoelectron energy going to ambient electrons as a result of Coulomb collisions.

$f_\lambda^{O(^1D)}$ = fraction of photoelectron energy used in the excitation of atomic oxygen to $^1D$ state and thereby causing 6300 Å airglow emission.

Since $O(^1D)$ atoms are in metastable state (with life-time of 110 sec), some of the energy which is initially spent in the excitation is returned to the neutral gas due to collisional quenching. The term $f_\lambda^{O(^1D)}$ should therefore be multiplied by a factor $(1 - f_Q)$ where $f_Q$ is the fraction of energy returned to the neutral atmosphere due to collisional deactivation. The expression for $f_Q$ is given in the next section. It is sufficient to state here that below 200 km, where most of the photoelectron energy goes to the neutral atmosphere, the value of $f_Q$ is generally close to unity (Izakov and Morozov, 1970). Thus in considering the thermospheric energy budget the term containing $f_\lambda^{O(^1D)}$ in Eq. 1, may be omitted without any serious error. We have also neglected photoelectron escape loss, since such nonlocal effects are small below 350 km (Geisler and Bowhill, 1965, Stubbe, 1971).

In calculating the thermal energy associated with photo-ionization as given by Eq. 1, we have assumed the photon flux and the ionization and absorption cross sections as given by Hinteregger et al (1965). In doing so, we have assumed that the ions are created in the ground state. Such an assumption implies that we might have somewhat overestimated the thermal energy from photoionization. This assumption was made partly because of the uncertainties in the ionization cross sections of the various excited states and partly because of the difficulty in making a realistic assessment of the energy available from the excited ions before and during their recombination. Numerical estimates using the table given by Nagy et al (1969) for probability of occurrence of various excited ionic states during photoionization, shows that about 10-20% reduction in photoelectron energy may result if we allow for production of these excited ions without their collisional quenching.

The term containing $f_\lambda^e$ which represents the energy imparted to the thermal plasma as a result of the Coulomb interaction, has been calculated by assuming an effective electron heating efficiency as given by Dalgarno et al (1968).

## PHOTO-DISSOCIATION

The most efficient photo-dissociation process in the atmosphere is that of $O_2$ molecules in the Schumann-Runge (S-R) continuum (1250-1750 Å). The photon energy in excess of the $O_2$-dissociation potential is shared by the O-atoms produced which may be in excited states. The excitation energy may be partially lost due to spontaneous radiation, and partially recovered through collisional de-excitation (metastable quenching). Following Izakov and Morozov (1970), the photo-dissociation heat input rate ($Q_d$) may be calculated from the following expression:

$$Q_d = [O_2] \int_{\lambda = 1250}^{1750} \epsilon_{O_2 \lambda}^{d} \sigma_{O_2 \lambda}^{a} F_{\lambda\infty} e^{-\tau_\lambda} d\lambda \qquad (2.a)$$

where $\epsilon_{O_2 \lambda}^{d}$ is the spectral heating efficiency of dissociation and may be written as

$$\epsilon_{O_2 \lambda}^{d} = \frac{\epsilon_\lambda - \epsilon_d}{\epsilon_\lambda} \qquad (2.b)$$

$\epsilon_d$ is the effective threshold energy for $O_2$ dissociation and is equal to 5.1 ev if oxygen atoms are produced in the (3 $p_2$) state. In general both O ($^3$p) and Q ($^1$D) atoms are produced in the process of dissociation and this requires an additional 1.96 ev. Since O ($^1$D) atoms are in metastable state (life-time 110 sec) they return some of their energy to the neutral gas through collisional deactivation. We may thus write

$$\epsilon_d = 5.11 + 1.96 (1 - f_Q) \qquad (2.c)$$

where $f_Q$ is the fraction of excitation energy returned to the neutral atmosphere due to collisional deactivation and may vary between 0-1 (from no quenching to complete quenching case). Izakov and Morozov (1970) have considered the collisions between O ($^1$D) and the three principal constituents of the neutral atmosphere) O, $O_2$ and $N_2$. They have considered an additional possibility that the collisions between O and $O_2$ may result in metastable $O_2$ (b $^1\Sigma_g^+$) which may loose part of its energy due to spontaneous emission. Noting that the energy of $O_2$ (b $^1\Sigma_g^+$) is equal to 1.64 ev, and assuming a quasi-stationary situation in the production and loss of O ($^1$D) and $O_2$ (b $^1\Sigma_g^+$), we may write:

$$f_Q = \frac{\sum_j K_j^{O(^1D)} n_j + K_b [O_2] \left\{ 1 + 0.84 \left( \frac{\sum_j K_j^{O_2(b)} n_j}{A_b + \sum_j K_j^{O_2(b)} n_j} - 1 \right) \right\}}{A_{^1D} + K_b [O_2] + \sum_j K_j^{O(^1D)} n_j} \tag{2.d}$$

where $A_{^1D}$ and $A_b$ are the Einstein coefficients for spontaneous radiation from O ($^1$D) and $O_2$ (b $^1\Sigma_g^+$), respectively; $K_a^{O(^1D)}$ and $K_a^{O_2(b)}$ are their quenching coefficients, $K_b$ is the rate coefficients for the production of $O_2$ (b $^1\Sigma_g^+$) and summation is carried over neutrals (O, $O_2$, $N_2$) effective in quenching. The numerical values of these coefficients adopted in our calculation are as follows (Izakov and Morozov, 1970)

$$K_j^{O(^1D)} = 1.6 \times 10^{-13},\ 1.0 \times 10^{-11},\ 5.0 \times 10^{-11} \text{ cm}^3 \text{ sec}^{-1}$$

and

$$K_j^{O_2(b)} = 1.0 \times 10^{-15},\ 9.0 \times 10^{-16},\ 1.5 \times 10^{-15} \text{ cm}^3 \text{ sec}^{-1}$$

for j corresponding to O, $O_2$, $N_2$, respectively; $A_{^1D}^{-1} = 110$ sec and $A_b^{-1} = 145$ sec.

## CHEMICAL ENERGY

A certain number of ions produced as a result of photo-ionization ultimately recombine with electrons and are lost. In the thermospheric region, the molecular ions [$O_2^+$, $NO^+$ and $N_2^+$] are lost as a result of dissociative recombination. In the case of atomic oxygen ions, this process is preceded by ion-atom interchange. Since dissociative recombination losses are generally exothermic, the ionic losses are usually accompanied by gain of thermal energy for the neutral constituents. The chemical energy or the heat input rate as a result of dissociative recombination can be calculated from the following expression

$$Q_r = \sum_k \alpha_k n_k^+(z) N_e(z) \Delta E_k \tag{3}$$

where $N_e$ (z) is the electron density at an altitude z; $n_k^+$ (z), $\alpha_k$ and $\Delta E_k$ are respectively ion density ($O_2^+$, $NO^+$ and $N_2^+$), rate coefficient and energy yield per reaction. Because the neutral atoms are produced in different excited states, $\Delta E_k$ may vary over a wide range. In our calculations, we have used average values for the most probable set of reactions, which are respectively 3.69, 1.31 and 3.14 ev for $O_2^+$, $NO^+$, and $N_2^+$.

## ENERGY TRANSFER FROM ELECTRONS AND IONS

Due to lack of thermodynamic equilibrium between thermal plasma and the neutral gas, there is a net energy transfer from the electrons and ions to the neutral particles via elastic and inelastic collisions. The ions lose most of their energy to the neutral gas via elastic collisions. The electrons, however, lose their energy to the neutral particles via the following processes [Banks 1966 (a, b), 1967: Dalgarno and Degges, 1968; Herman and Chandra 1969 (a, b); Stubbe, 1971].

(1) Elastic collisions with O, $O_2$, $N_2$, NO, H and He.

(2) Vibrational excitations of $O_2$ and $N_2$.

(3) Rotational excitations of $O_2$ and $N_2$.

(4) Electronic excitation of atomic oxygen to $^1D$ State.

(5) Fine structure excitations of atomic oxygen to $3P_1$ and $3P_0$ states.

For normal ionospheric conditions, the most important loss process is the fine structure excitation of O, and the least important is elastic collisions. The excitation energies may again be partially lost via radiative de-excitation. A steady population of certain excited species (e.g., $N_2$ vibrational state) may also exist according to Boltzmann distribution. However, these aspects have only small secondary effects on overall neutral heating problem and are ignored here.

## NEUTRAL WIND ENERGY

The transfer of energy between thermal plasma and the neutral atmosphere takes place not only because of the lack of thermodynamic equilibrium but also because of their relative motions [Stubbe and Chandra, 1971]. The neutral wind arising from the global pressure variations tends to move the electron-ion gas. Due to resistive action of the geomagnetic field in perpendicular direction, the ions exert a resistive drag on the neutrals. As a result of their mutual interactions the thermal energy received by the neutral gas is given by the following expression

$$Q_w = \sum_j n_j \sum_k \frac{m_j m_k^2}{(m_j + m_k)^2} \nu_{jk} (\vec{v}_k - \vec{v}_j)^2 \qquad (4)$$

where n, m, $\nu$ and $\vec{v}$ represent the number density, mass, collision frequency and velocity, respectively, and the subscripts j and k stand for the neutral and ionic constituents, respectively. The numerical computation of Eq. (4) is based on the values of collision frequencies given by Stubbe (1968).

## INFRARED RADIATION

In the preceding sections, we have described the various forms of energy which contribute to the heating of the neutral atmosphere in the thermospheric region. The primary source of these various forms of energy, of course, is the solar ultraviolet radiation which manifests itself in different forms through a complex chain of processes of interaction with the neutral atmosphere. The sink of thermal energy is the atomic oxygen, though in the lower thermosphere and the mesosphere $CO_2$ may provide an important cooling agent. In our calculations, we have only considered cooling associated with the 63 $\mu$ emission by O which is given by the following expression (Bates, 1951):

$$Q_L = [O] \frac{1.67 \times 10^{-18} \exp(-228/T_n)}{1 + 0.6 \exp(-228/T_n) + 0.2 \exp(-325/T_n)} \text{ ergs cm}^{-3} \text{ sec}^{-1} \qquad (5)$$

In a given volume, the conduction and convection processes also act as sources of cooling or heating. In a closed system, however, they do not constitute as a true energy sources or sink, since their role is only to redistribute energy.

## METHOD OF CALCULATIONS

Figure 1 summarizes, qualitatively, the various heat sources and sinks described in the preceding sections and their mutual relationships. They represent a complex system of closely coupled processes.

In order to study the relative importance of the various source and sink mechanisms outlined above and their role in affecting the thermal structure and kinematics of the upper atmosphere, we solve the basic heat conduction equation of the neutral gas

$$\sum_j C_{vj}\, \rho_j \frac{d T_n}{d t} + p \nabla \cdot \vec{v} = Q_T - Q_L + Q_C \tag{6}$$

with

$$\frac{d}{dt} = \frac{\partial}{\partial t} + \vec{v} \cdot \frac{\partial}{\partial \vec{r}}$$

In Eq. (6), $C_{vj}$ is the specific heat at constant volume and $\rho_j$ the mass density of the jth neutral constituent; $Q_T$ and $Q_L$ are the heat input and loss rates respectively, p and $\vec{v}$ denote the neutral gas pressure and velocity, respectively.

While $Q_L$ is clearly identified with radiation loss rate given by (5), $Q_T$ is given by the sum

$$Q_T = Q_i + Q_d + Q_r + Q_p + Q_w \tag{7.a}$$

where $Q_i$, $Q_d$, $Q_r$, $Q_p$ and $Q_w$ are heat input rates associated, respectively, with photoelectrons, photo-dissociation, dissociative recombination (chemical), plasma-neutral exchange, and neutral wind as discussed in the preceding sections.

The last quantity $Q_C$ on the right hand side of Eq. (6) represents the contribution of molecular conduction due to a non-vanishing temperature gradient of the thermosphere region. Neglecting horizontal temperature gradients, we have

$$Q_C = -\nabla \cdot (-\lambda_C \nabla T_n) = \frac{\partial}{\partial z}\left(\lambda_C(z) \frac{\partial T_n}{\partial z}\right) \tag{7.b}$$

where $\lambda_C$ is the molecular conductivity. We have chosen the following model of the conductivity [Dalgarno and Smith, 1962 (a, b); Tsederberg, 1965]

$$\lambda_C(z) = \frac{\sum_j B_j\, n_j(z)\, T_n^{b_j}}{\sum_j n_j(z)} \tag{7.c}$$

with the values of the various parameters $B_j$ and $b_j$ shown in Table 1.

Table 1

Coefficients of Conductivity Model

| Constituent (j) | $B_j$ | $b_j$ |
|---|---|---|
| $O_2$ | 18.64 | 0.84 |
| $N_2$ | 27.21 | 0.80 |
| O | 67.10 | 0.71 |
| H | 16.36 | 0.73 |
| He | 20.92 | 0.75 |

The second term on the left side of Eq. (6) represents the mechanical energy associated with the expansion and contraction of the atmosphere. Using the equations of state and continuity, the terms on the L.H.S. can be combined and Eq. (6) can be expressed in the following form

$$\sum_j C_{pj}\, \rho_j \frac{dT}{dt} - \frac{dp}{dt} = Q_T - Q_L + Q_C \tag{8}$$

where $C_{pj}$ = specific heat at constant pressure. In the altitude region above 120 km, the atmosphere may be assumed to be in diffusive equilibrium. Provided the horizontal pressure gradients are much smaller compared to the vertical gradient, one is led, as a direct consequence of these assumptions and the equations of continuity and state, to the following relations:

$$\frac{dp}{dt} = 0 \tag{9.a}$$

and,

$$v_{jz}(z) = \frac{T_n(z)}{g(z)} \int_{z_0}^{z} \frac{g(z')}{T_n^2(z')} \frac{\partial T_n(z')}{\partial t} dz' + \frac{H(z)}{p(z_0)} \frac{\partial p(z_0)}{\partial t} \tag{9.b}$$

The solution of Eq. (8) is carried out in conjunction with simultaneous solution of the following equations:

(1) Equations of continuity of $O_2^+$, $NO^+$, $O^+$, $H^+$

(2) Heat conduction equations of $O^+$, $H^+$ and electron gas

(3) Equations of motion for X and Y components of the neutral gas.

These equations constitute a set of 10 coupled partial differential equations, of first order in time and second order in space coordinates, with appropriate assumptions to justify a one dimensional description of the system. The details of these equations and their method of solution has been described in detail by Stubbe (1970) and will not be repeated here.

The neutral constituents (O, $O_2$, $N_2$, He and H) are assumed to be in diffusive equilibrium with the values of O, $O_2$ and $N_2$ densities specified at 120 km and the values of H density specified at 500 km according to the U.S. Standard Atmosphere (supplement, 1966). The value of He density is specified at 500 km according to the form given by Keating et al (1970). The boundary condition for the neutral temperature is as follows:

at 1500 km : $\partial T_n / \partial z = 0$

at 120 km : $T_n = 355°K$

The numerical results presented in this paper are for mid-latitude ($\lambda$ = 42.6°N) and for the solar flux values as given by Hinteregger et al. (1965). These fluxes were originally suggested by Hinteregger to correspond to the solar minimum condition. Recently, however, a new set of fluxes with somewhat different spectral distribution and generally lower intensity, has been given by Hinteregger (1970) to correspond to the solar medium conditions. Thus the flux-values used in this calculation are comparatively high, and may correspond to a medium to high solar activity.

## HEATING AND COOLING RATES

Various heating and cooling rates for typical daytime conditions are shown in Fig. 2. We observe that the dissociation heating rate, $Q_d$, is the most dominant mechanism below about 160 km. The contribution due to photoelectrons, $Q_i$, is seen to be the most important heating mechanism for the altitude range of about 170-500 km. Above this range, low neutral densities combined with high Coulomb transfer rate, effectively reduce the importance of this term. At these altitude, however, increased electron and ion temperatures induce relatively higher plasma neutral energy exchange. The neutral wind heating rate, $Q_n$, is roughly a factor of 2 smaller than the plasma neutral exchange rate, $Q_p$, both peaking at about 180 km. The chemical (electron-ion recombination) heat input rate, $Q_r$, is generally comparable to the exchange rate $Q_p$ for lower altitudes ($z \lesssim 300$ km), but is negligibly small at higher altitudes. Finally, the radiation loss due to infrared emission, shown in Fig. 2 by the dashed curve, is observed to be generally small at most altitudes. During night-time, however, this contribution is quite significant, particularly at lower altitudes ($z \lesssim 300$ km), as shown in Fig. 3.

It is of interest to calculate the height-integrated heat-source and sink contributions for a vertical column of the atmosphere of unit cross section. This is easily done by integrating the basic heat conduction Eq. (6). The result is shown in Fig. 4. From the figure, the predominance of the photo-dissociation of $O_2$ in the S-R continuum for thermospheric heating is evident, as is the role of thermal molecular conduction from the lower boundary at 120 km. Photoelectron energy is an important source during daytime, as expected, but its contribution is less than the dissociation energy.

The plasma feedback energy shown in Fig. 4 is the sum of the chemical, plasma-neutral exchange and neutral wind heat input rates integrated over a vertical column, and this sum is seen to be relatively a small source during daytime. During nighttime on the other hand, the combined contribution of these processes has a low enough value to be regarded as almost negligible in comparison with conduction and radiation losses. Furthermore, since this additional (plasma feedback) energy is in phase with the photo-dissociation and photoelectron energies, the explicit inclusion or exclusion of this term in the energy balance equation does not change the phase of the neutral temperature. It, however, does affect the magnitude of the exospheric temperature by about 20%.

The thermal conduction loss of energy from the lower boundary at 120 km (bottom curve of Fig. 4) is seen to be quite large and to exhibit a diurnal variation in approximate antiphase with the exospheric temperature $T_\infty$ variation, with maximum and minimum around 0600 and 1600 hrs LT, respectively. In contrast $T_\infty$ has a minimum around 0600 and a maximum around 1700 hrs, LT. Finally, the mechanical energy ($\int p \nabla \cdot \vec{v}\, dz$) (related to the expansion and contraction of the atmosphere) acts as a heat source in the night time and sink in the day time. Over 24 hours, its total contribution is zero; therefore, it does not constitute a real heat source or sink for the system as a whole.

## HEATING EFFICIENCY

Having discussed the importance of the various heat sources, we can now estimate their heating efficiencies. The heating efficiency, which by definition is the fraction of absorbed ultraviolet energy available as heat energy is, in fact, a function of wavelength and depends upon the spectral distribution of radiation, cross sections, and the type of processes under consideration. For the thermospheric calculations, however, we may define two efficiencies corresponding to photo-ionization and photo-dissociation. In defining a photo-ionization heating efficiency we may include the terms arising from dissociative recombination, plasma neutral exchange and neutral wind. This is possible since the total energy from the plasma feedback (Fig. 4) varies in phase with the photoelectron energy. Our estimate of the photo-ionization heating efficiency gives values between 0.5-0.6. However, we prefer the value 0.5 in view of the fact that we have overestimated the photoelectron energy in our calculation. This value may be used down to 110 km. Below this altitude region, the photo-ionization rate and hence the photo-ionization efficiency becomes negligibly small. The heating efficiency corresponding to photo-dissociation is found to be 0.33 for lower altitudes, reducing to a value of 0.1 at higher altitudes ($z \gtrsim 450$ km). With the absorption in the S-R continuum and the dissociation heating rate reducing drastically at higher altitudes, the decrease of heating efficiency in this region may be ignored without any serious error. Thus a general value of 0.3 as suggested by Izakov (1971) is quite reasonable.

## SUMMARY AND CONCLUDING REMARKS

In this paper we have attempted to assess the relative importance of the various heat sources arising as a result of the interaction of the solar ultraviolet with the atmospheric constituents above 120 km. In view of the numerical complexity of the problem which involved solving a large number of time dependent coupled integro-differential equations, we chose to make certain simplifying assumptions. For example, we did not consider the role of excited ions nor did we consider all the radiative de-excitation and exothermic reactions individually. Thus we may have slightly over-estimated the thermal energy directly available from photoelectrons and underestimated the energy available from chemical heating. We may nevertheless arrive at the following conclusions from this study:

(1) The thermal energy available from S-R continuum is comparable to (or, for lower boundary below 120 km, even greater than) all the energy sources combined. Since the photo-dissociation energy is proportional to the $O_2$ density, seasonal changes in $O_2$ density in the lower atmosphere will have considerable effect on the thermospheric structure.

(2) Since the total energy from the plasma (including chemical, dynamical and thermodynamical processes) is in phase with the photoelectron energy, it does not change the basic diurnal pattern of thermospheric temperature (the time of the temperature maximum and minimum).

Thus it does not constitute a basically different heat source and is not a substitute to the controversial second heat source introduced by Harris and Priester (1962).

(3) The most significant loss rate for the altitude region above 120 km is the downward thermal conduction ultimately resulting in a net heat loss across the lower boundary to the region below. Detailed calculations to study the effect of changing the lower boundary have indicated that the thermal conduction loss rate from the lower boundary and its diurnal characteristic are strongly dependent on the choice of the parameters of the lower boundary.

In general, the lower boundary parameters have a profound effect on the diurnal characteristics of the thermospheric temperature and densities. For example, a change in temperature at 120 km from 325°K to 500°K may change the diurnal amplitude of the exospheric temperature from 1.5 to 1.3. The diurnal variations in the neutral constituents at 120 km affect directly their phases with respect to the exospheric temperature (Stubbe and Chandra, 1970). In principle, therefore, it seems desirable to choose the boundary at a lower altitude where changes in the boundary parameters and their effect on the thermal structure may be minimal. The importance of choosing a lower height as the lower boundary for the study of the thermospheric heat budget problem is even more evident once we realize that a rather significant portion of the photo-dissociation energy is available below 120 km. From the point of solving the thermal conduction equation, the most natural boundary is the mesopause level where we can assume zero conduction ($\partial T/\partial z = 0$). Thus the altitude region above the mesopause can be treated as a thermally insulated system where almost all the solar ultraviolet energy is absorbed and where a significant part of the thermal energy is lost via 62 $\mu$ emission by atomic oxygen at lower thermospheric heights. The role of atomic oxygen in the energy balance of the thermosphere is particularly important since it is produced by the same process (photo-dissociation of $O_2$) which produces the dominant thermal energy. Because of the self-regulatory nature of the heating and cooling rates, we have undertaken the study of the energy balance problem along with the equations of continuity of the atmospheric constituents. We hope that this study would provide a self-consistent model of the density and temperature of the upper atmosphere and would help in understanding the observed temporal and seasonal changes in the thermospheric region.

## ACKNOWLEDGEMENTS

One of us (A. K. S.) was supported by NASA under grant no. NSR 21-002-096.

# REFERENCES

Banks, P. (1966a). Planet. Space Sci. 14, 1085

Banks, P. (1966b). Planet. Space Sci. 14, 1105

Banks, P. (1967). J. Geophys. Res. 72, 3365

Bates, D. R. (1951). Proc. Phys. Soc. (B) 64, 805

Chandra, S. and Stubbe, P. (1970). Planet. Space Sci. 18, 1021

Dalgarno, A. and Smith, F. J. (1962). Planet. Space Sci. 9, 1

Dalgarno, A. and Smith, F. J. (1962). Proc. Roy. Soc. A 267, 417

Dalgarno, A. and Degges, T. C. (1968). Planet. Space Sci. 16, 125

Dalgarno, A., McElroy, M. B., Rees, M. H. and Walker, J. C. G. (1968). Planet. Space Sci. 16, 1371

Geisler, J. E. and Bowhill, S. A. (1965). J. Atmo. Terr. Phys. 27, 457

Hanson, W. B. and Johnson, F. S. (1961). Mem. Soc. Roy. Sci. Liege 5, 390

Harris, I. and Priester, W. (1962). J. Atm. Sci. 19, 286

Herman, J. R. and Chandra, S. (1969a). Planet. Space Sci. 17, 1247

Herman, J. R. and Chandra, S. (1969b). Planet. Space Sci. 17, 815

Hinteregger, H. E., Hall, L. A. and Schmidtke, G. (1965). Space Res. V. 1175-1190, North Holland, Amsterdam.

Hinteregger, H. E. (1970). Ann. Geophys. 26, 547

Hunt, D. C. and Van Zandt, T. E. (1961). J. Geophys. Res. 66, 1673.

Izakov, M. N. (1971). Space Sci. Rev. 12, 261

Izakov, M. N. and Morozov, S. K. (1970). Geomagnetism and Aeronomy 10, 495

Lagos, C. P. and Mahoney, J. R. (1967). J. Atm. Sci., 24, 88

Lazarev, W. I. (1963). Geomagnetizm i aeronomija 3, 841. NASA Draft Translation ST-AT 10094 (1964)

Keating, F. M., Mullins, J. A. and Prior, E. J. (1970). Space Res. X., North Holland, Amsterdam

Nagy, A. F., Fontheim, E. G., Stolarski, R. S. and Beutler, A. E. (1969). J. Geophys. Res. 74, 4667

Nicolet, M. (1961). Planet. Space Sci., 5, 1

Stubbe, P. (1968). J. Atm. Terr. Phys. 30, 1965

Stubbe, P. (1970). J. Atm. Terr. Phys. 32, 865

Stubbe, P. (1971). Indian J. Sci. Industr. Res. 30, 379

Tsederberg, N. V. (1965). Thermal Conductivities of Gases and Liquids, MIT Press.

# THERMOSPHERIC ENERGETICS

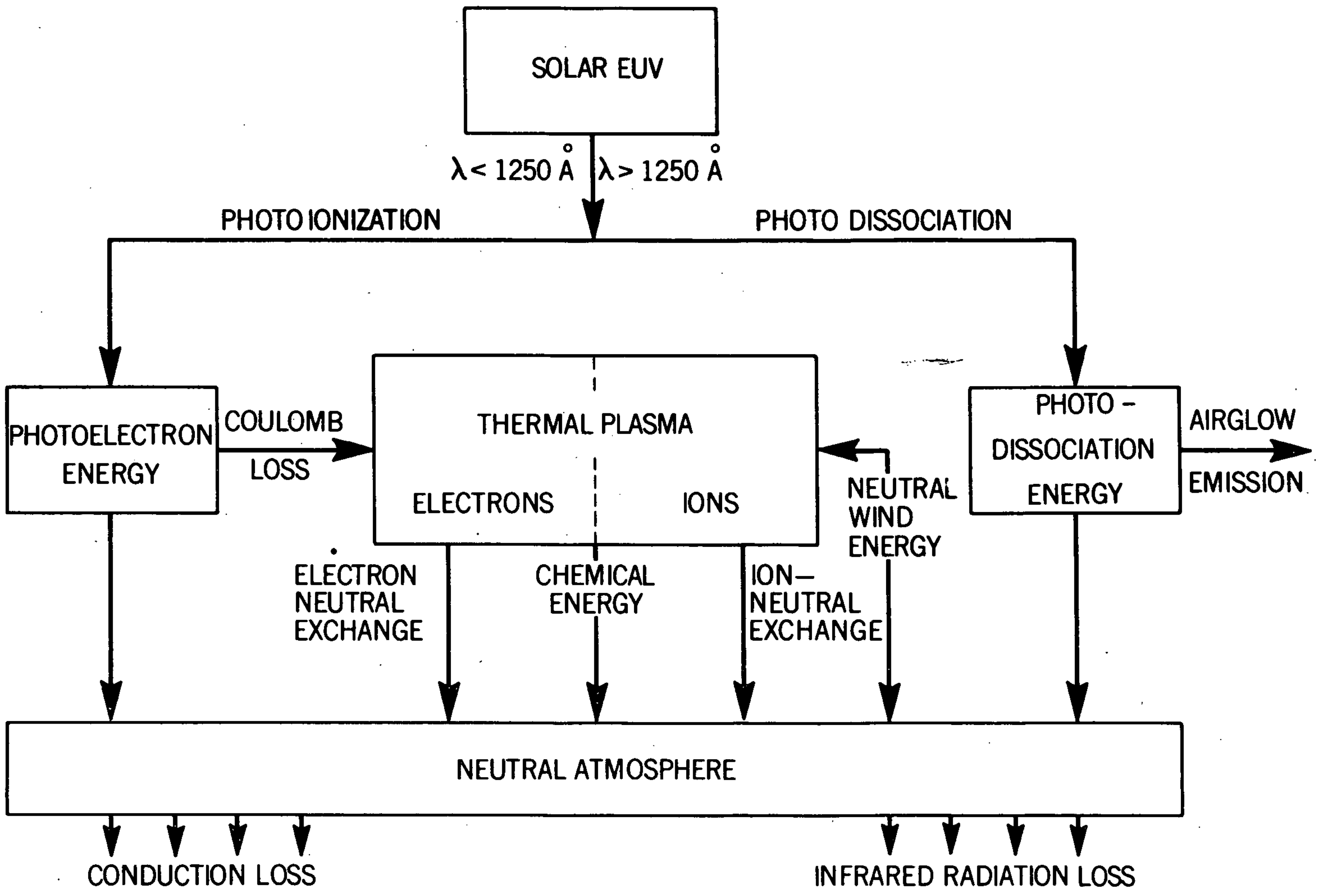

Figure 1. Schematic Representation of the Basic Processes of Thermospheric Heating

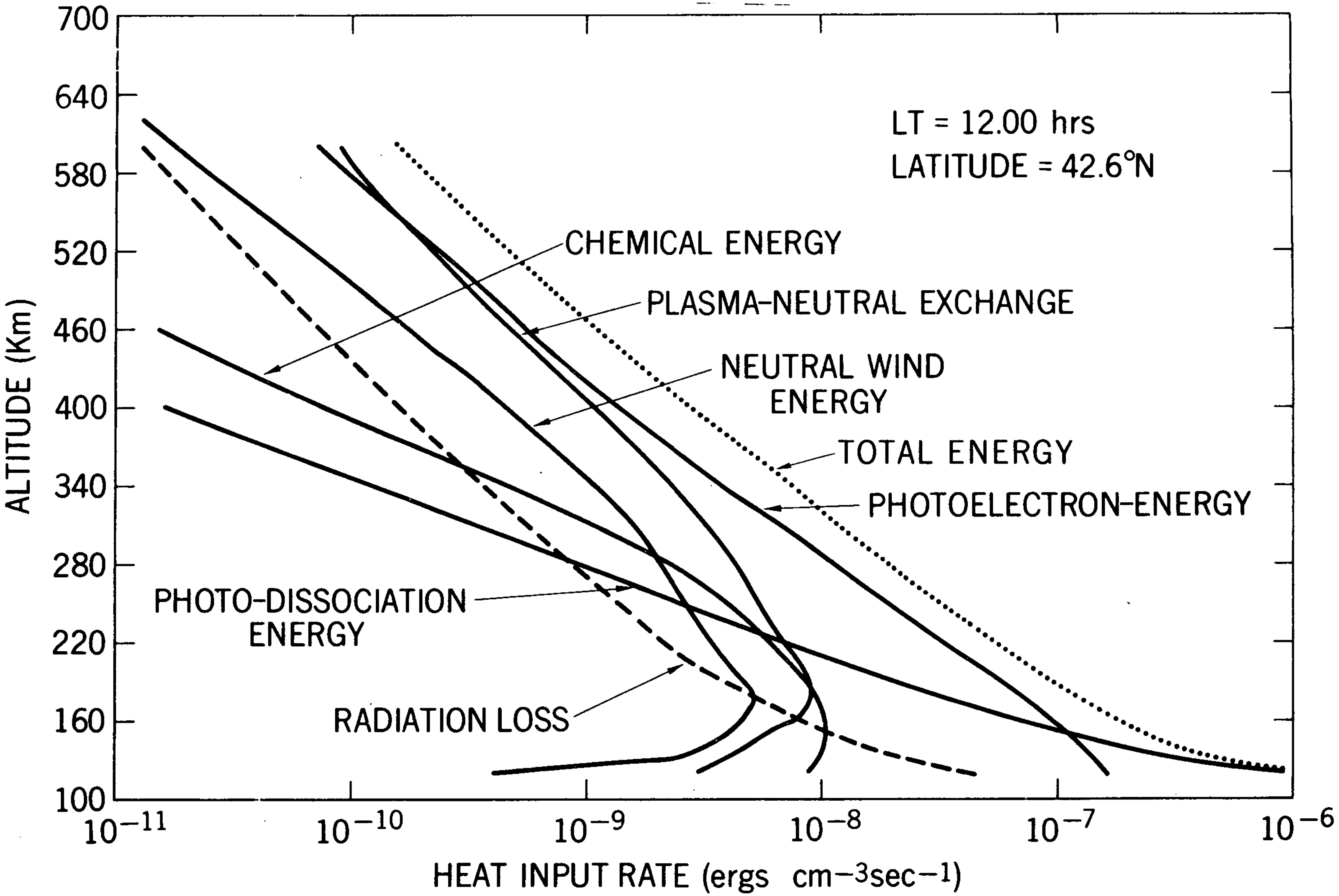

Figure 2. Heating (Solid Curves) and Cooling (Dashed Curves) Rates vs. Altitude for Different Processes at Local Noon

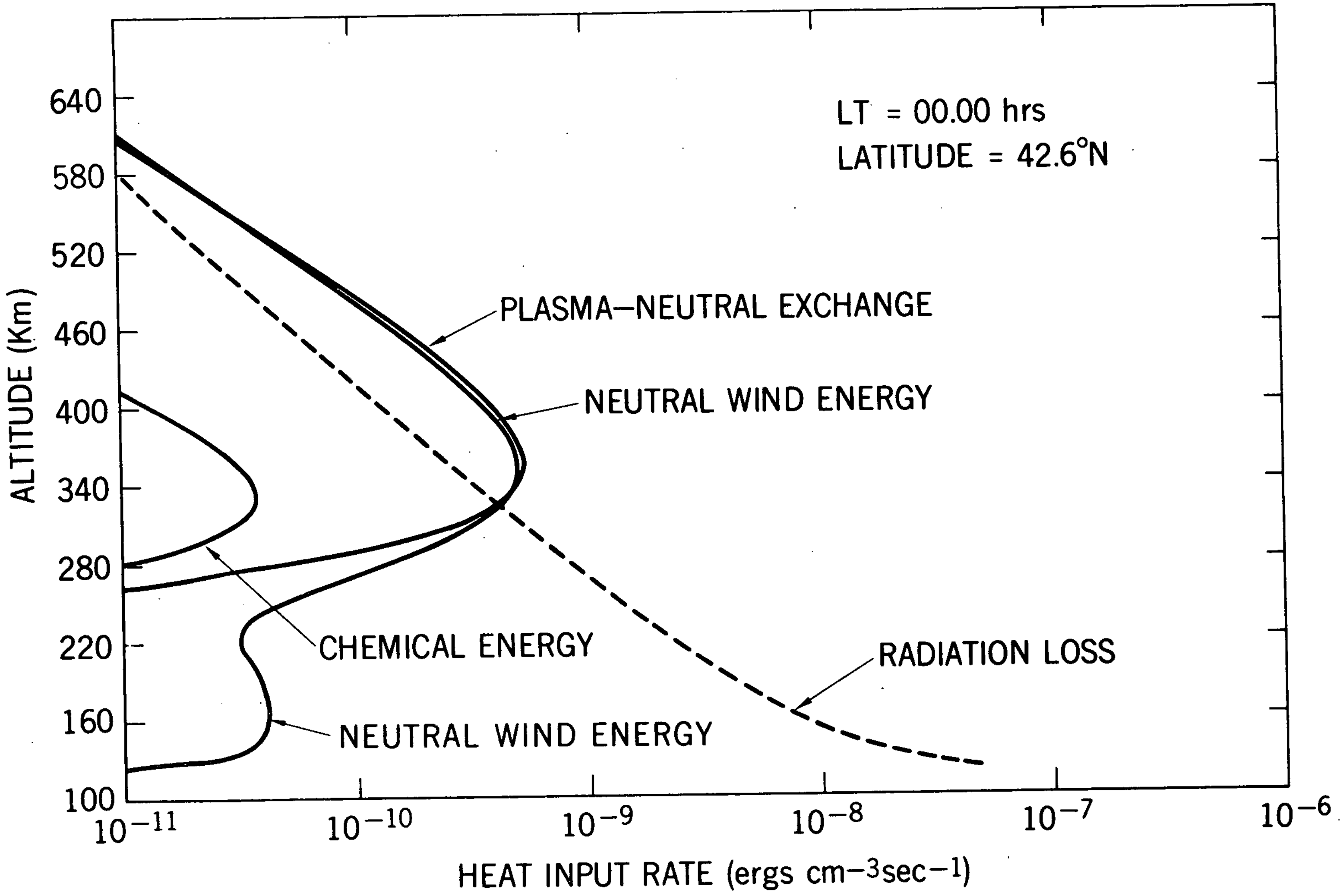

Figure 3. Heating (Solid Curves) and Cooling (Dashed Curve) Rates vs. Altitude for Different Processes at Local Midnight

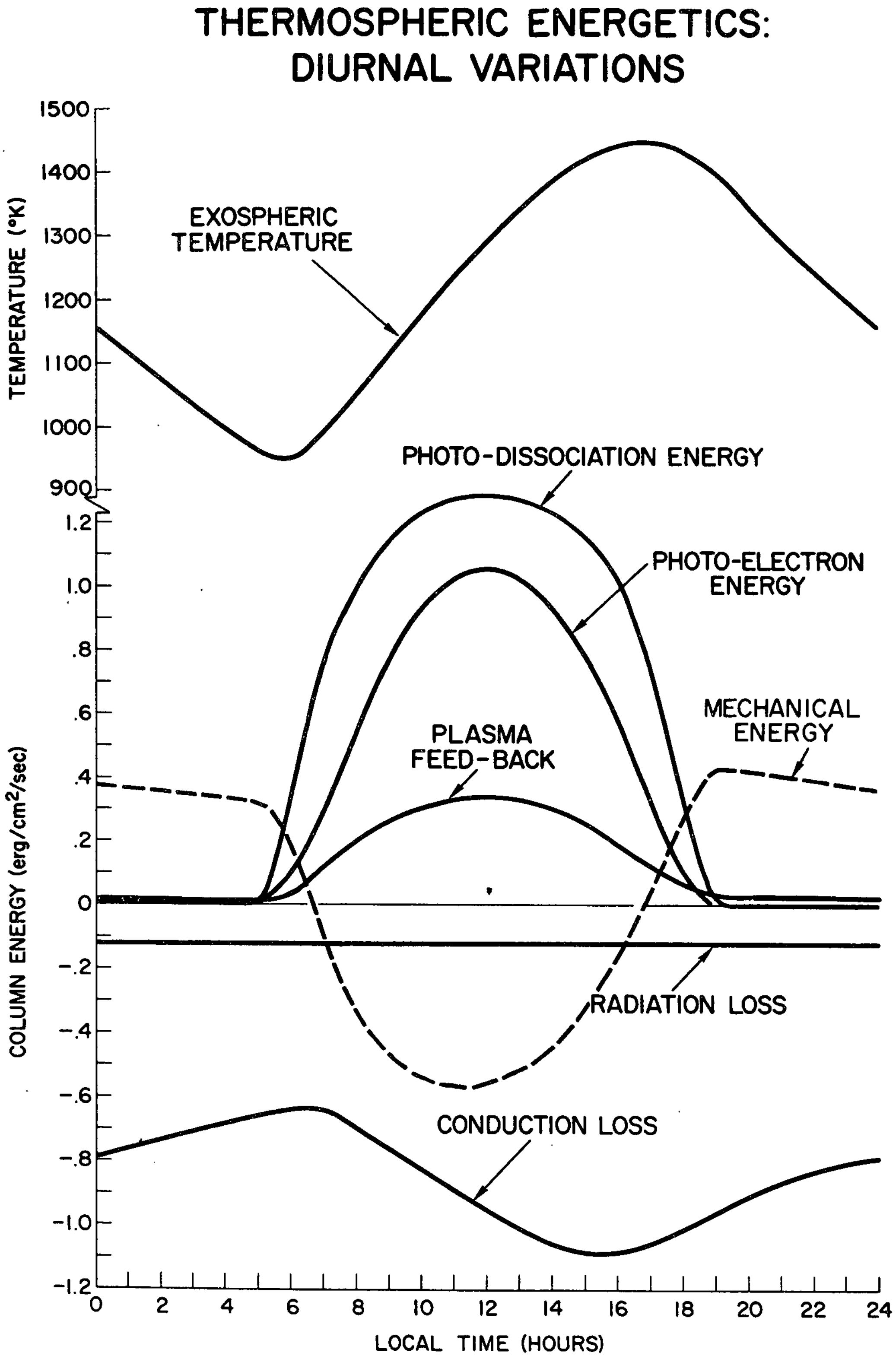

Figure 4. Diurnal Variation of Altitude-Integrated Heat Input and Loss Rates for a Vertical Column of Atmosphere of Unit Cross-Section Above 120 km